GDCh

Research Articles

Angewandte
Chemie
International Edition
www.angewandte.org

Small Molecule Activation | Hot Paper |

Synthesis and Reactivity of a Neutral Homocyclic Silylene

Jan Keuter, Alexander Hepp, Anja Massolle, Johannes Neugebauer,
Christian Mück-Lichtenfeld, and Felicitas Lips*

Dedicated to Professor Matthias Drieß on the occasion of his 60th birthday

Abstract: *Isolation of the neutral homocyclic silylene **2** is possible via amine ligand abstraction with potassium graphite (KC₈) and subsequent reaction with SiMe₃Cl from a bicyclic silicon(I) amide **J**. This reaction proceeds via an anionic homoaromatic silicon ring compound **1** as an intermediate. The twofold-coordinated silicon atom in the homocyclic silylene **2** is stabilized by an allyl-type π-electron delocaliza-tion. **2** reacts in an oxidative addition with two equivalents of MeOH and in cycloadditions with ethene, phenylacetylene, diphenylacetylene and with 2,3-dimethyl-1,3-butadiene to afford novel functionalized ring compounds.*

Introduction

Silicon analogues to carbenes, i.e. silylenes[1] have recently emerged as reactive species in main group element based small molecule activation.[2] For instance, silylenes can provide oxidative addition with H_2 and NH_3 under mild conditions.[3] Some reactions of silylenes with suitable reagents also proceed reversibly such as the addition of ethene.[4] Furthermore, an equilibrium reaction between silicon species in the formal oxidation state +II and +IV was observed in an intramolecular reaction of a silylene with an aryl substituent to form a sila-cycloheptatriene (silepin) **A** (Figure 1). This system can activate H_2, CO_2 and ethene.[3a]

Silylenes are also utilized as ligands in transition metal complexes for catalysis due to their strong donor ability.[5] Especially, heterocyclic silylenes such as amino(bora-ylide)[6] **D** and amino(phospha-ylide) stabilized silylenes[7] **E** are stronger σ-donors than *N*-heterocyclic carbenes and conven-tional phosphines such as P'Bu₃ and PPh₃ (Figure 1).
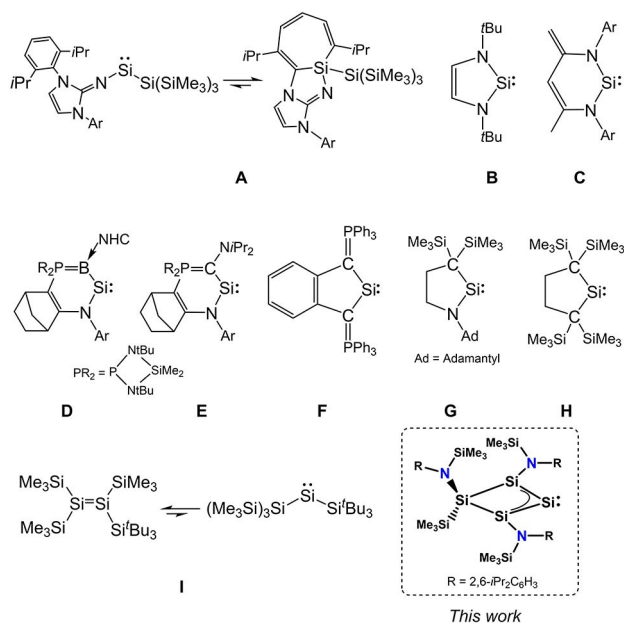

Figure 1. Isolable heterocyclic silylenes **B–H** and acyclic silylenes **A** and **I** that are in equilibrium with Si^IV species. Ar = 2,6-*i*Pr₂C₆H₃).

Synthetic access to cyclic and acyclic silylenes[3,8] has become very broad after the report on the first *N*-heterocyclic silylenes (**B**, **C**).[9] In both types of silylenes different substituents can be introduced primarily via silicon-(IV)halides and reductive dehalogenation. For instance, in heterocyclic silylenes besides bora-ylides in **D**[6] and phos-pha-ylides in **E**[7] and **F**,[10] a combination of alkyl and amine in **G**[11] and alkyls in **H**[12] were utilized. The synthesis of an acyclic bis(silyl)substituted silylene **I**[13] (Figure 1) was recently reported that is in equilibrium with a disilene compound via a silyl group migration. This compound reacts with H_2 under very mild conditions (hexane, −40 °C). However, the synthesis of an isolable neutral homocyclic silylene that features only silicon atoms connected to the twofold-coordinated silicon atom has not been reported so far.

Results and Discussion

We obtained access to a homocyclic silylene in an unconven-tional two-step procedure by 1) the reduction of **J**[14] with 2 equiv. of KC₈ in the presence of [18]crown-6 leading to the

[*] Dr. J. Keuter, Dr. A. Hepp, Dr. F. Lips
Westfälische Wilhelms-Universität Münster, Institut für Anorgani-sche und Analytische Chemie
Corrensstraße 28–30, 48149 Münster (Germany)
E-mail: lips@uni-muenster.de

A. Massolle, Prof. J. Neugebauer, Dr. C. Mück-Lichtenfeld
Westfälische Wilhelms-Universität Münster, Organisch-Chemisches Institut and Center for Multiscale Theory and Computation
Corrensstraße 36, 48149 Münster (Germany)

elimination of K{N(SiMe₃)Dipp}. This reaction affords an anionic silicon ring compound **1** that in step 2) in the subsequent reaction with SiMe₃Cl yields the homocyclic silylene **2** in form of orange-red crystals (Method A, Scheme 1).

Alternatively, the formation of **2** is possible directly from **J** by *in situ* generation of **1·K⁺** and addition of two equiv of SiMe₃Cl. In this case the amine N(SiMe₃)₂Dipp was identified as the side product (Method B, Scheme 1). This synthesis of the homocyclic silylene **2** starting from a four-membered neutral or anionic precursor is a novel approach for the access of silylenes.

Compounds **1** (Figure 2) and **2** (Figure 3) were comprehensively characterized with single crystal X-ray diffraction,[15] NMR and UV/Vis spectroscopy, ESI mass spectrometry, DFT (TPSS-D3/def2-TZVP)[16] and broken symmetry[17] calculations.

The cleavage of one amine substituent from **J** affords **1** with a folded four-membered silicon ring with two amine substituents oriented above the Si₄-plane and one amine positioned below this plane. The latter amine is bound to

the trigonal pyramidal Si3 atom ($\Sigma\sphericalangle$Si3: 278.64(2)°). The other two amine substituents bind to the two trigonal planar Si2 and Si4 atoms ($\Sigma\sphericalangle$Si2: 357.97(3)°, $\Sigma\sphericalangle$Si4: 358.08(3)°). The two-fold coordinated Si1 atom has a small Si2-Si1-Si4 bond angle of 65.21(4)°. This bond angle is significantly smaller than that in other cyclic silylenes (92.6–99.3°) because Si1 is incorporated into a rhombic four-membered ring and not in a five-membered ring as in the case of **B**, **F**–**H**.

In the ²⁹Si NMR spectrum the pyramidal Si3 atom has a chemical shift of $\delta^{29}Si = 96.7$ ppm. This resonance is very unusual for the configuration of Si3. But chemical shifts in the downfield region were reported for fourfold-coordinated silicon atoms in siliconoids[18] and for the central silicon atom of the allyl-type system in the cyclotetrasilenide [Si₄(SiMe*t*Bu₂)₃(*t*Bu)₂]⁻.[19] The two trigonal planar Si2 and Si4 atoms resonate at $\delta^{29}Si = 220.0$ ppm. The Si1 atom displays a signal in the downfield region at $\delta^{29}Si = 437.9$ ppm which is in the range of acyclic amido(boryl) and amido-(silyl)silylenes.[3b,c] The measured chemical shifts for **1** in THF-d_8 are in very good agreement with those calculated for the DFT-optimized structure **1-opt** (Table S3).

The geometric and electronic properties within the Si₄ ring in **J** and in **1** differ considerably. The dihedral angle between the two three-membered rings in **J** (131.76°) is smaller than that in **1** (Si1–Si2–Si4–Si3: 159.86°). Thus the Si4 ring in **1** approaches planarity compared to **J**. Although the distance between the trans-annular silicon atoms Si2 and Si4 in **1** is almost identical to that in **J**, we found that no covalent σ-bond exists between these atoms in **1**. This is confirmed by their low field signals in the ²⁹Si NMR spectrum ($\delta = 220.0$ ppm). In this downfield region usually signals of silyl cations are recorded such as for [Et₃Si-(benzene)]⁺ ($\delta = 92.3$ ppm)[20] and for [Mes₃Si]⁺ ($\delta = 225.5$ ppm).[21] This underlines the unsaturated character of Si2 and Si4 in **1**. Furthermore, quantum theory of atoms in molecules (QTAIM)[22] reveals the absence of a bond critical point between these two atoms (Figure S37). This is in
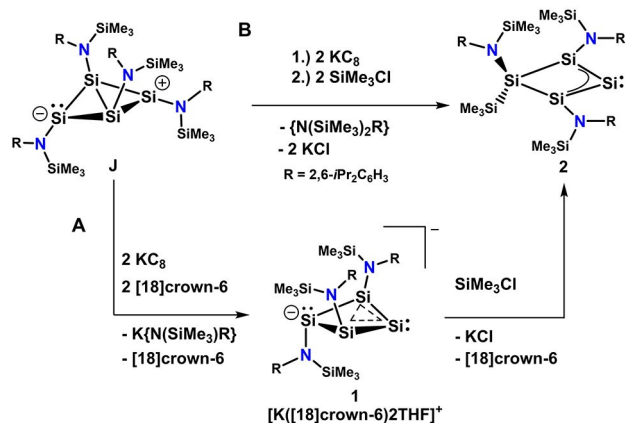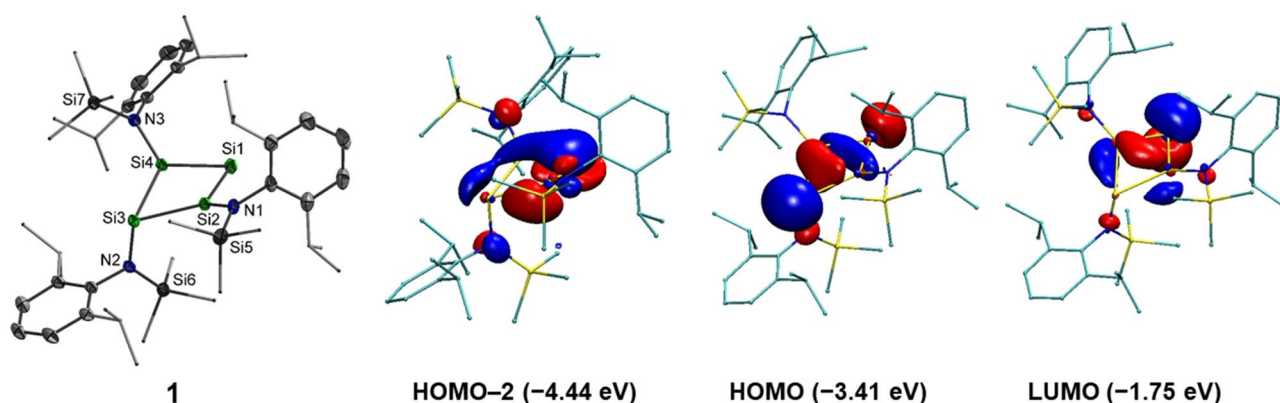
Scheme 1. Synthesis of **1** and **2**.

Figure 2. Left: Molecular structure of **1**. Thermal ellipsoids are set at 50% probability level. H atoms are not shown. Selected bond lengths [Å] and angles [°] for **1**: Si1–Si2 2.274(8), Si2–Si3 2.411(8), Si3–Si4 2.447(8), Si4–Si1 2.275(8), Si2···Si4 2.451(8), Si1···Si3 3.951(1), Si2–N1 1.766(2), Si3–N2 1.848(2), Si4–N3 1.774(2); Si2-Si1-Si4 65.21(3), Si2-Si3-Si4 60.60(2), N1-Si2-Si4 149.75(7), N3-Si4-Si2, 151.11(7), Si1-Si2-Si4-Si3 159.864(5). Center and Right: Frontier molecular orbitals of **1-opt** with orientation of the molecule identical to that shown on the left (TPSS-D3/def2-TZVP, Isovalue set at +/− 0.05 a.u.).
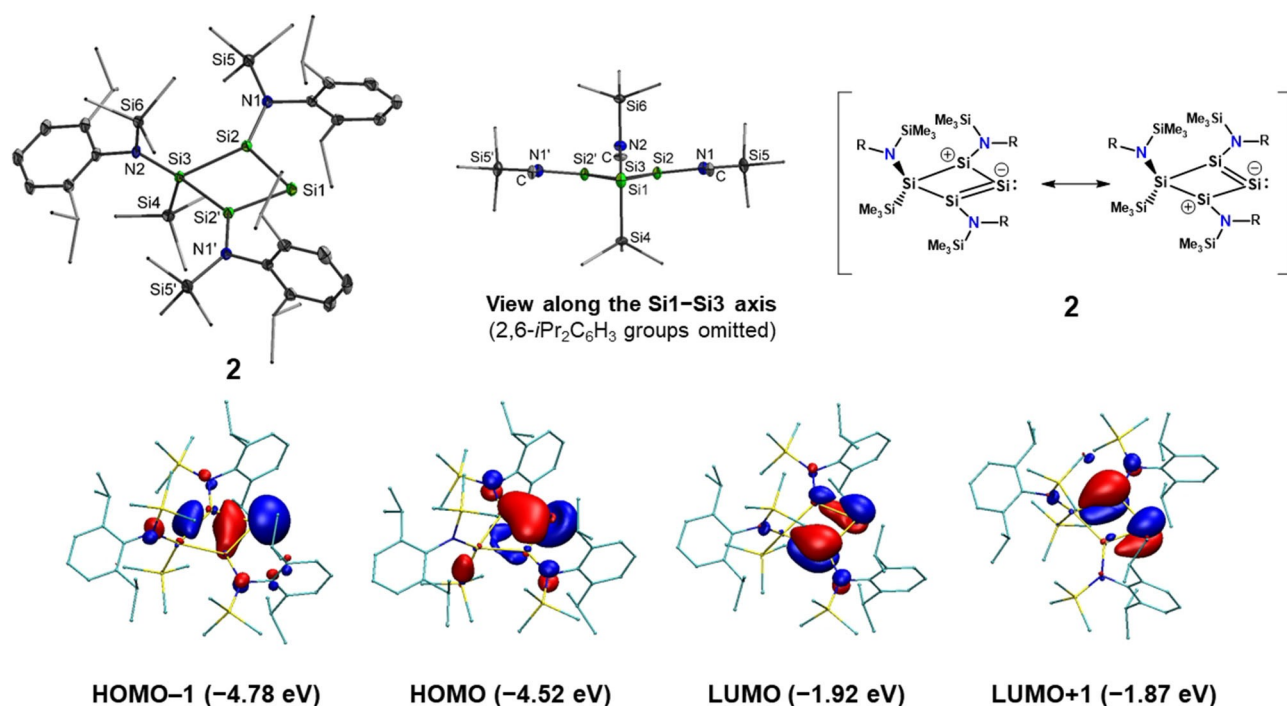
Figure 3. Top: Molecular structure of **2**. Thermal ellipsoids are set at a 50% probability level. H atoms are not shown. Selected bond lengths [Å] and angles [°] for **2**: Si1–Si2 2.248(9), Si2–Si3 2.408(1), Si3–Si4 2.400(5), Si2⋯Si2′ 2.682(1), Si1⋯Si3 3.779(1), Si2–N1 1.750(2), Si3–N2 1.759(3), Si2-Si1-Si2′ 73.24(4), Si1-Si2-Si3 108.44(3), Si2-Si3-Si2′ 67.69(4), N1-Si2-Si2′ 167.72(6), Si1-Si2-Si2′-Si3 166.633(2). Bottom: Frontier molecular orbitals of **2-opt** with orientation of the molecule identical to that shown on the left (TPSS-D3/def2-TZVP, Isovalue set at +/− 0.05 a.u.).

contrast to the bonding situation found for **J** with a bond critical point located at the bridgehead bond (Figure S38) and with signals for the bridgehead atoms appearing at much higher field in the ^{29}Si NMR spectrum ($\delta = 57.6$ and 58.5 ppm) than those of **1**. Additionally, the HOMO−1 of **J** (TPSS-D3/def2-TZVP)[16] entails the σ-bond between these atoms. Investigations of the molecular orbitals of **1** (TPSS-D3/def2-TZVP) reveal the absence of such a bond. Instead, π-type electron delocalization takes place at Si1, Si2 and Si4 in the HOMO-2. This hints towards a three-center two-electron (3c–2e) π-bond involving these silicon atoms in **1**, represented with a dashed line in Scheme 1.

Nucleus independent chemical shift (NICS(0)) calculations[23] at the center of the three-membered ring formed by Si1, Si2 and Si4 reveals a highly negative value of $\delta = -25$ ppm (Supporting Information Page S32) which is smaller than that of benzene ($\delta = -9.7$) ppm and confirms this finding.

Furthermore, NBO analysis[24] of a model compound **1H** with N(SiH$_3$)H substituents revealed a 3c–2e π-bond located between Si1, Si2 and Si4 (Table S8). The short Si1–Si2 and Si1–Si4 bonds (2.274(8) and 2.275(8) Å) that are in the upper range of Si=Si double bonds (2.14–2.29 Å)[25] underline their partial double bond character that is caused by the 3c–2e π-bond. Additionally, σ-type lone pairs are found at Si1 and Si3 in the HOMO with a larger contribution at Si3. The LUMO of **1** comprises an empty p-type orbital at Si1 and indicates a 1,3-orbital interaction involving Si2 and Si4 (Figure 2 and S36). Thus, **1** can be considered as an anionic

homoaromatic compound in which homoconjugation occurs which is the reason for the folded Si4 ring in **1**. Only a few silicon-based homoaromatic compounds were reported such as the homocyclo-trisilenylium cation [Si$_4$(SiMe^{t}Bu$_2$)$_3$-(^{t}Bu)$_2$]$^+$,[26] the molybdenum and tungsten complexes [M-(Cp)$_2${Si$_4$(SiMetBu$_2$)$_4$}] (M=Mo, W; Cp= cyclopentadienyl)[27] and the siliconoid cluster Si$_5$(Trip)$_6$ (Trip=2,4,6-iPr$_3$C$_6$H$_2$).[28] Investigation of **1** with a broken symmetry approach[17] demonstrates that **1** has closed shell singlet character while triplet and/or open-shell singlet states are energetically disfavored (Supporting Information Pages S37, S50–S52).

Reaction of **1**·[K([18]crown-6)·2THF] with SiMe$_3$Cl at −20 °C in THF results in the addition of the SiMe$_3$ group at the trigonal pyramidal Si3 atom under release of the salt KCl and [18]crown-6. This reaction affords the neutral orange-red silicon compound **2** with a rhombic four-membered ring in 85% yield (Scheme 1). In contrast to **J** and **1**, the rhombic Si$_4$ ring in **2** is almost planar with a sum of internal bond angles of 357.81(2)°.

Additionally, in **2**, the nitrogen atoms connected to Si2 and Si2′ are arranged almost in plane to the rhombic Si$_4$ unit but feature bond lengths of 1.750(2) Å that are only 0.02 Å shorter than those in **1**. Thus, they are still in the lower range of Si–N single bonds.[29]

In **2**, depicted in Figure 3, the two-fold coordinated Si1 atom is retained and displays a larger Si–Si–Si bond angle of 73.24(4)° compared to that in **1** (65.21(3)°). This is related to the increased transannular distance between Si2 and Si2′

(2.682(1) Å) in **2** which is 0.23 Å longer than that in **1**. Similar to **1**, the Si2 and Si2′ atoms in **2** are trigonal planar with sum of surrounding bond angles of 359.80(1)°. These atoms resonate in the downfield region at 225.3 ppm which is similar to the situation in **1**. The two-fold coordinated Si1 atom in **2** forms short bonds to Si2 and Si2′ (2.248(9) Å) that are in the upper range of Si=Si double bonds (2.14–2.29 Å).[25] These bonds are only slightly shorter (0.03 Å) than those in **1** (2.274(8) and 2.275(8) Å) and indicate partial double bond character. ^{29}Si NMR spectroscopy of **2** revealed a resonance of the twofold-coordinated Si1 atom at 195.0 ppm (Table S10). This signal is shifted by 243 ppm to higher field compared to the corresponding resonance of Si1 in **1**. This suggests that a different type of π-electron delocalization is dominating in **2** compared to the 3c–2e π-bond in **1** which is also indicated by the larger transannular distance between Si2 and Si2′ in **2**.

Compared to the carbocyclic silylene **H**[12] (δ = 576.4 ppm), the resonance for the twofold-coordinated silicon atom in **2** is shifted to higher field. However, the signal is in the region of that of the acyclic amido-substituted thermally unstable silylene Si{N(SiMe$_3$)$_2$}$_2$ (δ = 223.9 ppm),[30] the sterically crowded acyclic boryl-amido substituted silylene Si{N(SiMe$_3$)(DAB)}$_2$ (δ = 204.6 ppm, DAB = B-(DippNCH)$_2$, Dipp = 2,6-iPr$_2$C$_6$H$_3$)[3d] and the phospha-ylide-stabilized carbocyclic silylene **F** (δ = 212.4 ppm).[10]

The UV/Vis absorption spectrum of **2** in *n*-hexane exhibited a distinct absorption band at λ_{max} = 400 nm arising from the HOMO→LUMO transition as indicated by TD-DFT calculations (Page S14). A second absorption at λ_{max} = 365 nm is associated to the transition HOMO→LUMO+1. The wavelengths of these absorption bands are between the longest wavelength absorption band of **H** (λ_{max} = 440 nm)[12] and that of **B** (λ_{max} = 292 nm).[9]

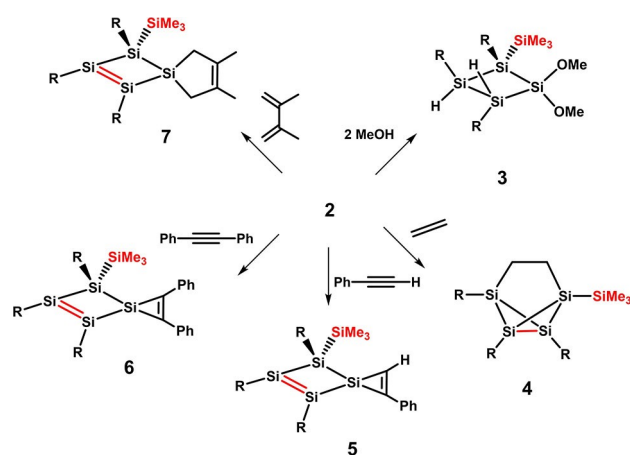The bonding situation in **2** was elucidated applying molecular orbital theory, NBO[24] and NPA[31] analysis with DFT on **2-opt**. The HOMO−1 contains the σ-type lone pair at Si1. Atom orbitals of π-symmetry delocalized at Si1/Si2 and Si1/Si2′ with the main contribution at Si1 are visible in the HOMO. In accordance with the observed Si–N single bond lengths the molecular orbitals of **2-opt** confirm the absence of Si=N double bond character. This suggests that the N atoms carry p-type lone pairs of electrons that allow for the occurrence of negative hyperconjugation into the antibonding σ*-orbitals of the Si–Si bonds. The LUMO and LUMO+1 include empty p-type orbitals at Si1/Si2 and Si1/Si2′, respectively (Figure 3 and Figure S41). They do not show any 1,3-orbital interaction between Si2 and Si2′ in contrast to the LUMO of **1**. This indicates that an allyl-type π-electron delocalization is dominating in **2**. This situation is related to that in the cationic Si$_4$ ring compound [{Si$_3$(tBu)$_2$-(SiMetBu$_2$)}{Si(tBu)$_2$}]$^+$ with allylic character.[32] Consequently, **2** can be represented with the resonance structures shown in Figure 3.

Wiberg bond indices (WBI)[33] of **2-opt** support the partial double bond character of the Si1–Si2/Si2′ bonds which have bond orders of 1.28/1.26 and are thus somewhat higher than the Si–Si single bonds from Si2/Si2′ to Si3 (0.92) in **2-opt** (Table S12). The WBI (0.55) for the transannular

Si2···Si2′ distance in **2-opt** is lower than that of **1-opt** (0.74). Similar to the case of **1-opt**, no bond critical point was found with Bader's quantum theory of atoms in molecules between these transannular atoms in **2-opt** (Figure S42). Investigations of **2** with a broken symmetry approach[17] demonstrates that **2** has also closed shell singlet character despite the almost planar four-membered ring. For **2** triplet and/or open-shell singlet states are energetically disfavored (Supporting Information Pages S48, S52–S54).

Calculated partial charges for **2** with natural population analysis (NPA)[31] revealed a negative partial charge of −0.17 for Si1 and positive partial charges of +0.64 and +0.63 for Si2 and Si2′ and of +0.40 for the four-coordinate Si3 atom of the four-membered silicon ring. Thus, in contrast to the *N*-heterocyclic silylene **C** (+1.26), the cyclic (amino)phospha-ylide substituted silylene **E** (+1.00) and the cyclic (amino)-bora-ylide substituted silylene **D** (+0.65) the Si1 atom carries a negative partial charge. This suggests that **2** is electron-rich and features nucleophilic character. NBO analysis[24] of a model compound of **2** indicates the presence of a formally "empty" p-orbital at Si1 (occupancy with 0.64 e$^-$) besides a lone pair of σ-character at Si1 (Table S13). A partially occupied (0.54 e$^-$) formally "empty" p-orbital was also observed with NBO analysis for the *N*-heterocyclic silylene **B**.[34] Due to the dominating allyl-type character involving Si1, Si2 and Si2′ in **2**, the empty p-orbital at Si1 is partially filled and stabilized. These spectroscopic and computational data indicate the formation of the first isolable neutral homocyclic silylene. This type of silylene was previously only observed as an intermediate,[35] and a dicationic base-coordinated silicon ring compound was isolated that may be considered as a cationic base-stabilized homocyclic silylene.[36]

Silylene **2** does not react with dihydrogen even at elevated temperatures of 80 °C and a pressure of 1 bar. But **2** undergoes reactions with ethene, 2,3-dimethyl-1,3-butadiene, phenyl- and diphenylacetylene and methanol to yield **3**–**7** (Scheme 2 and Figure 4/Figure 5).[15] In the reaction with two equiv. methanol a completely saturated four-membered ring species **3** was obtained in a two-fold oxidative addition. The reaction with ethene affords the unusual tricyclic

Scheme 2. Reactivity of **2**, R = N(SiMe$_3$)Dipp.

Angew. Chem. Int. Ed. **2022**, *61*, e202114485 (4 of 8)

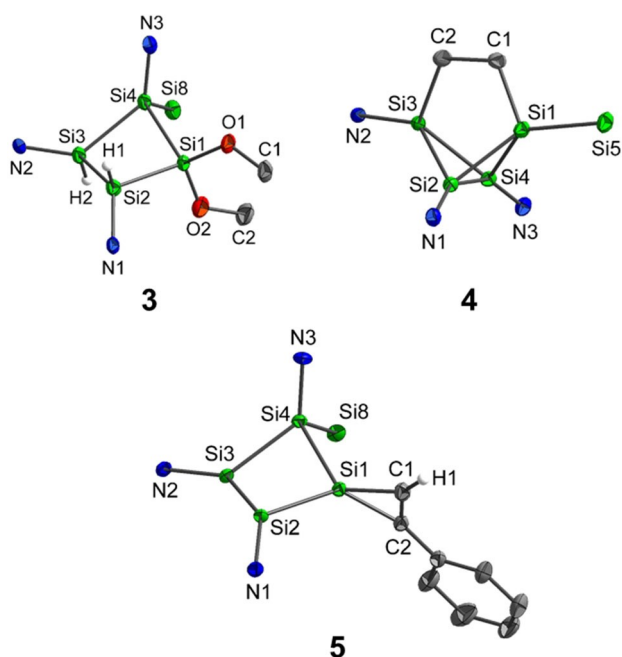© 2021 The Authors. Angewandte Chemie International Edition published by Wiley-VCH GmbH

Figure 4. Cutouts of molecular structures 3–5. Thermal ellipsoids are set at a 50% probability level. SiMe₃ and Dipp groups are not shown. Selected bond lengths [Å] for **3**: Si1–O1 1.633(4), Si1–O2 1.643(4), Si1–Si2 2.3709(19), Si2–Si3 2.3831(19), Si3–Si4 2.4266(19), Si4–Si1 2.4026(18), Si4–Si8 2.392(2), Si1···Si3 3.114(2), Si2···Si4 3.468(2). For **4**: Si1–Si2 2.3649(8), Si2–Si3 2.4178(7), Si3–Si4 2.3914(8), Si4–Si1 2.3638(8), Si2–Si4 2.3493(8), Si1···Si3 2.9819(2), Si1–C1 1.922(2), Si3–C2 1.896(2), C1–C2 1.504(3). For **5**: Si1–Si2 2.2840(11), Si2–Si3 2.2302(11), Si3–Si4 2.3634(11), Si4–Si1 2.3640(11), Si1···Si3 3.0701(1), Si2···Si4 3.328(1), Si1–C1 1.818(3), Si1–C2 1.838(3), C1–C2 1.331(5).
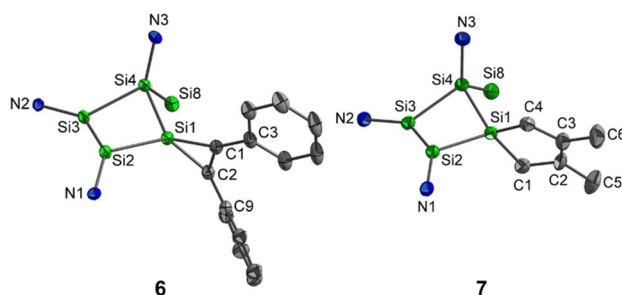

Figure 5. Cutouts of molecular structures 6 and 7. Thermal ellipsoids are set at a 50% probability level. SiMe₃ and Dipp groups are not shown. Selected bond lengths [Å] For **6**: Si1–Si2 2.3025(9), Si2–Si3 2.2600(8), Si3–Si4 2.3705(8), Si4–Si1 2.3729(9), Si1···Si3 3.1195(1), Si2···Si4 3.370(1), Si1–C1 1.840(2), Si1–C2 1.839(2), C1–C2 1.341(3). For **7**: Si1–Si2 2.3021(15), Si2–Si3 2.2193(15), Si3–Si4 2.3642(16), Si4–Si1 2.3815(15), Si1···Si3 3.1579(2), Si2···Si4 3.278(2), Si1–C1 1.893(5), C1–C2 1.523(7), C2–C3 1.322(7), C3–C4 1.506(6), Si1–C4 1.903(5).

saturated ring species **4**. Cycloadditions with acetylenes and 2,3-dimethyl-1,3-butadiene yield unsaturated bicyclic ring compounds **5–7**.

In the reactions of **2** with MeOH, phenylacetylene, diphenylacetylene and 2,3-dimethyl-1,3-butadiene shown in Scheme 2 a formal 1,2-silyl shift occurs. Formation of **4**, from **2** and ethene is accompanied by a 1,3-silyl migration.

This suggests that isomers of **2** with the corresponding migrated silyl group might occur in solution. For this reason, we performed temperature-dependent NMR (210 K to 360 K in THF-d_8/PhMe-d_8) (Figure S27) and UV/Vis spectroscopy (25°C to 150°C in PhMe, and at −150°C to 25°C in 2-methylpentane (Figures S14, S15). Both experiments do not show any evidence for an equilibrium between **2** and a corresponding tetrasilacyclobutene **2′** or the constitutional isomer **2″** in solution (see Figure 6).

In contrast to previously known silylenes the oxidative addition of **2** with methanol proceeds not only once but twice and is accompanied by the formal 1,2-silyl-migration to yield **3**. By reacting only one equivalent of methanol with **2**, we attempted to isolate a possible intermediate. However, this reaction results in the formation of the product **3** besides unreacted **2** (see Figure S61). This suggests that the intermediate is more reactive than **2**. A selective reaction with only two equiv. of methanol was previously also observed with unsaturated silicon species such as a tetrasilabicyclo[1.1.0]butene, an unsymmetrically substituted disilene, a trisilaallene and a disilyne.[37]

The products of **2** with the alkynes correspond to [2+1] cycloadditions and that with 2,3-dimethyl-1,3-butadiene to a [4+1] cycloaddition. This reaction behavior is known for silylenes[38] and therefore confirms the silylene character of **2**. The Si=Si double bonds between Si2 and Si3 in **5–7** were confirmed by the short bond lengths (2.219(2)–2.260(8) Å) and their downfield chemical shifts in the ²⁹Si NMR spectrum (for **5**: 31.4 and 56.5 ppm for **6**: 38.8 and 52.9 ppm, and for **7**: 33.0 and 41.4 ppm). We propose that the reaction of **2** with ethene occurs via a [2+1] cycloaddition at the two-coordinate Si1 atom as the first step, which is typical for silylenes[39] and may primarily lead to a similar product as those observed with phenylacetylene and diphenylacetylene.

To shed light on these points, we explored the possible equilibrium between **2** and **2′** or **2″** and the reaction of **2** with ethene, phenylacetylene and methanol with a modified DFT procedure (PW6B95-D3//PBEh-3c+COSMO-RS)[40] shown in Figure 6, 7 and 8. 1,2-silyl migration transforming **2** to **2′** via **TSb(2-2′)** is kinetically disfavoured ($\Delta G^{\pm} = 51.9$ kcal mol^{-1}). A rearrangement of the Si₄ core through an almost tetrahedral transition structure via **TSa(2-2′)** (Figure S106) has a low barrier ($\Delta G^{\pm} = 22.8$ kcal mol^{-1}) and is slightly endergonic ($\Delta G(\mathbf{2} \rightarrow \mathbf{2′}) = +1.7$ kcal mol^{-1}), leaving the concentration of **2′** too low for NMR observation. Skeletal isomerizations were recently also discussed for a 1,3-dichlorobicyclo[1.1.0]tetrasilane.[41] Formation of the even less stable bicyclic isomer **2″** ($\Delta G(\mathbf{2} \rightarrow \mathbf{2″}) = 3.7$ kcal mol^{-1}) by 1,2-silyl shift from **2′** via **TS(2′-2″)** is kinetically unfavoured ($\Delta G^{\pm} = 36.1$ kcal mol^{-1}).

Considering these facts, we propose that the reaction of **2** with ethene initially occurs with its isomer **2′** via a [2+1] cycloaddition at the divalent Si1 atom. The barrier of formation of **Int1-4′** from **2′** is $\Delta G^{\pm} = 19.0$ kcal mol^{-1}, which is compatible with the experimental conditions and lower than the barriers of rearrangement to **2** or **2″**. Furthermore, formation of **Int1-4′** is slightly exergonic ($\Delta G = -4.8$ kcal mol^{-1}). This is different to the endergonic reaction to silacyclopropane **Int1-4** ($\Delta G = 6.1$ kcal mol^{-1}), which also
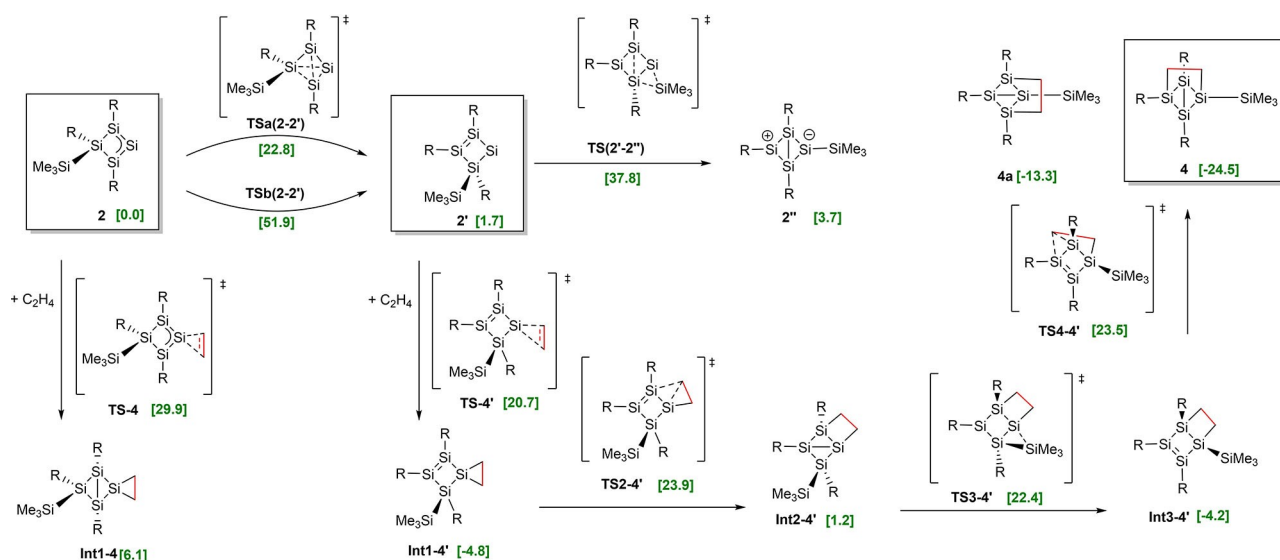
Figure 6. Calculated isomerization of **2/2′/2″** and intermediates and transition structures in the reaction of **2/2′** with ethene. In brackets: calculated free energies relative to isolated reactants (**2** and ethene) in kcal mol⁻¹.

has a higher activation barrier of ethene insertion of $\Delta G^{\ddagger} =$ 29.9 kcal mol⁻¹.

We further identified a viable reaction sequence which rationalizes the rearrangement of **Int1-4′** to the observed product **4** under the reaction conditions. Firstly, we identified a 1,2-alkyl shift with the highest barrier of $\Delta G^{\ddagger} =$ 28.7 kcal mol⁻¹ via **TS2-4′** to the intermediate **Int2-4′** representing the rate-determining step. This is followed by the 1,2-silyl shift which transfers the SiMe₃ group to the silylene center with a sufficiently low barrier via **TS3-4′** ($\Delta G^{\ddagger} =$ 21.2 kcal mol⁻¹). The second alkyl shift from **Int3-4′** to product **4** is irreversible due to the stability of **4**. An alternative ethylene-bridged product **4a** (Figure 6) which could be formed from **Int3-4′** is significantly less stable than **4**.

The situation is less clear in the reaction of **2** with phenylacetylene. Silacyclopropene **5** is the observed product, despite the fact that the rearranged tricyclic isomer **8**, depicted in Figure 7, is much more stable ($\Delta G(\mathbf{5}{\rightarrow}\mathbf{8}) =$ −27.7 kcal mol⁻¹). Obviously, the alkyne reacts with **2′**, since compound **9a** (Figure 7) or the diastereoisomer **9** (Figure S109) derived from **2** are not observed. The calculated barriers for addition of **2** and **2′** to the alkyne are similar and comparable to the barrier of isomerization. The isomer-
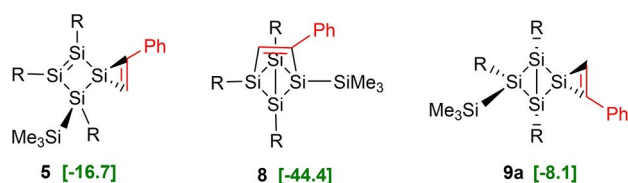
ization of **5** by opening of the silacyclopropene ring is kinetically disfavoured ($\Delta G^{\ddagger} > 32$ kcal mol⁻¹), prohibiting formation of **8** (see **TS1-5** and **Int1-5** in Figure S109 and Table S27).

The formation of the bis-methoxy product **3** from **2** and two methanol molecules is very exergonic ($\Delta G =$ −62.6 kcal mol⁻¹, Figure 8). Calculated activation barriers for the addition of one molecule of MeOH are too high to proceed under the reaction conditions (Figure S111). As in the previously discussed reactions, **2′** is more reactive towards the alcohol than **2** (Figure S110). Hydrogen bond assisted reaction of **2′** with two MeOH molecules lowers the barrier considerably (Figure 8). In this case, 1,1-addition via
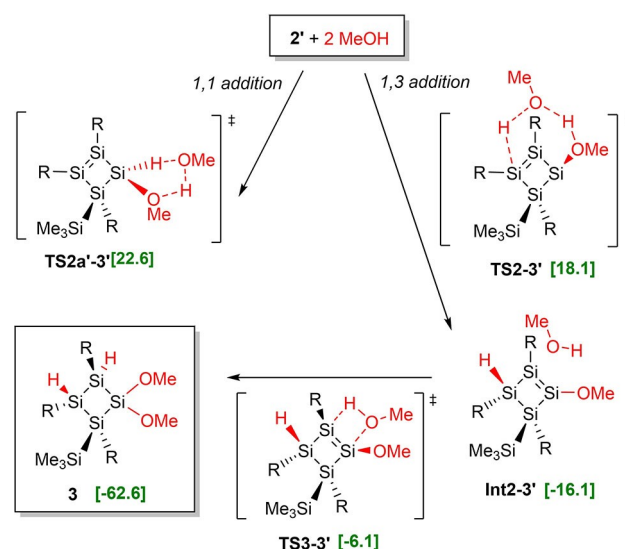

Figure 7. Calculated product **5** and hypothetical products **8** and **9a**. In brackets: calculated free energies relative to isolated reactants (**2** and phenylacetylene) in kcal mol⁻¹.

Figure 8. Calculated intermediates and transition states during the formation of **3**. In brackets: calculated free energies relative to isolated reactants (**2** and two MeOH molecules) in kcal mol⁻¹.

TS2a′-3′ is predicted to be slower than 1,3-addition via **TS2-3′**. Therefore, we propose that **Int2-3′** is formed with the methoxy group connected to the Si=Si double bond. This activates the Si=Si double bond for the subsequent 1,2-addition with another MeOH molecule. The low barrier of only 10 kcal mol⁻¹ via **TS3-3′** confirms the observation that the second equivalent of the alcohol reacts faster than the first one to yield the final product **3**.

The bicyclic ring compounds **5**–**7** contain a rare tetrasilacyclobutene moiety. Only a few tetrasilacyclobutenes are reported with silyl, alkyl, iodine and aryl substituents.[42] In general, the formation of the unsaturated tetrasilacyclobutene units in **5**–**7** can probably be traced back to reduced ring strain in unsaturated silicon rings compared to saturated species.[43] Moreover, compounds **5**–**7** can be classified as heterocyclic spiro compounds[44] that usually represent unique preparative challenges. However, the syntheses of **5** and **7** proceed via a simple cycloaddition route at room temperature from the homocyclic silylene **2/2′**.

Conclusion

In summary, we describe the formation of an anionic homoaromatic silicon ring compound **1** that is employed for the synthesis of a new type of silylene **2**. In the homocyclic silylene **2**, the two-coordinate silicon atom is part of an almost planar rhombic four-membered silicon ring. With the adjacent homoatomic atoms the silylene functionality features an uncommon negative partial charge which makes the silylene electron-rich with nucleophilic character.

Computational investigations show that a skeletal rearrangement within **2** affords a more reactive silylene **2′** that undergoes oxidative addition with two equivalents of MeOH and with ethene with lower activation barriers and yields energetically preferred intermediates **Int2-3′** and **Int1-4′**, respectively.

The reactivity of the homocyclic silylene was further probed in [2+1] cycloadditions with the alkynes phenylacetylene and diphenylacetylene to yield spiro-compounds **5** and **6**, and in a [4+1] cycloaddition with 2,3-dimethyl-1,3-butadiene to access spiro-compound **7**. The bicyclic ring compounds **5**–**7** comprise less strained tetrasilacyclobutene rings. The low-coordinate silicon atoms stabilized by the 3c–2e π-bond in the anionic homoaromatic compound **1** and the dominating allyl-type electron delocalization in the isolable homocyclic silylene **2** are highly promising tools for further reactions.

Acknowledgements

Conflict of Interest

The authors declare no conflict of interest.

Data Availability Statement

The data that support the findings of this study are available in the Supporting Information of this article.

[1] a) M. Haaf, T. Schmedake, R. West, *Acc. Chem. Res.* **2000**, *33*, 704–714; b) Y. Mizuhata, T. Sasamori, N. Tokitoh, *Chem. Rev.* **2009**, *109*, 3479–3511; c) M. Asay, C. Jones, M. Driess, *Chem. Rev.* **2011**, *111*, 354–396; d) B. Gehrhus, M. F. Lappert, J. Heinicke, R. Boese, D. Bläser, *J. Chem. Soc. Chem. Commun.* **1995**, 1931–1932; e) M. F. Lappert, A. Protchenko, P. P. Power, A. Seeber, *Metal Amide Chemistry*, Wiley, Chichester, **2009**, pp. 264–271.

[2] a) C. Weetman, S. Inoue, *ChemCatChem* **2018**, *10*, 4213–4228; b) T. Chu, G. I. Nikonov, *Chem. Rev.* **2018**, *118*, 3608–3680; c) P. P. Power, *Nature* **2010**, *463*, 171–177.

[3] a) D. Wendel, A. Porzelt, F. A. D. Herz, D. Sarkar, C. Jandl, S. Inoue, B. Rieger, *J. Am. Chem. Soc.* **2017**, *139*, 8134–8137; b) A. V. Protchenko, K. H. Birjkumar, D. Dange, A. D. Schwarz, D. Vidovic, C. Jones, N. Kaltsoyannis, P. Mountford, S. Aldridge, *J. Am. Chem. Soc.* **2012**, *134*, 6500–6503; c) V. Protchenko, A. D. Schwarz, M. P. Blake, C. Jones, N. Kaltsoyannis, P. Mountford, S. Aldridge, *Angew. Chem. Int. Ed.* **2013**, *52*, 568–571; *Angew. Chem.* **2013**, *125*, 596–599; d) T. J. Hadlington, J. A. B. Abdalla, R. Tirfoin, S. Aldridge, C. Jones, *Chem. Commun.* **2016**, *52*, 1717–1720.

[4] F. Lips, J. C. Fettinger, A. Mansikkamäki, H. M. Tuononen, P. P. Power, *J. Am. Chem. Soc.* **2014**, *136*, 634–637.

[5] a) Y.-P. Zhou, M. Driess, *Angew. Chem. Int. Ed.* **2019**, *58*, 3715–3728; *Angew. Chem.* **2019**, *131*, 3753–3766; b) B. Blom, D. Gallego, M. Driess, *Inorg. Chem. Front.* **2014**, *1*, 134–148.

[6] A. Rosas-Sánchez, I. Alvarado-Beltran, A. Baceiredo, N. Saffon-Merceron, S. Massou, V. Branchadell, T. Kato, *Angew. Chem. Int. Ed.* **2017**, *56*, 10549–10554; *Angew. Chem.* **2017**, *129*, 10685–10690.

[7] I. Alvarado-Beltran, A. Baceiredo, N. Saffon-Merceron, V. Branchadell, T. Kato, *Angew. Chem. Int. Ed.* **2016**, *55*, 16141–16144; *Angew. Chem.* **2016**, *128*, 16375–16378.

[8] a) M. M. D. Roy, M. J. Ferguson, R. McDonald, Y. Zhou, E. Rivard, *Chem. Sci.* **2019**, *10*, 6476–6481; b) B. D. Rekken, T. M. Brown, J. C. Fettinger, F. Lips, H. M. Tuononen, R. H. Herber, P. P. Power, *J. Am. Chem. Soc.* **2013**, *135*, 10134–10148; c) B. D. Rekken, T. M. Brown, J. C. Fettinger, H. M. Tuononen, P. P. Power, *J. Am. Chem. Soc.* **2012**, *134*, 6504–6507.

[9] M. Denk, R. Lennon, R. Hayashi, R. West, A. V. Belyakov, H. P. Verne, A. Haaland, M. Wagner, N. Metzler, *J. Am. Chem. Soc.* **1994**, *116*, 2691–2692.

[10] M. Asay, S. Inoue, M. Driess, *Angew. Chem. Int. Ed.* **2011**, *50*, 9589–9592; *Angew. Chem.* **2011**, *123*, 9763–9766.

[11] T. Kosai, S. Ishida, T. Iwamoto, *Angew. Chem. Int. Ed.* **2016**, *55*, 15554–15558; *Angew. Chem.* **2016**, *128*, 15783–15787.

[12] M. Kira, S. Ishida, T. Iwamoto, C. Kabuto, *J. Am. Chem. Soc.* **1999**, *121*, 9722–9723.

[13] D. Reiter, R. Holzner, A. Porzelt, P. J. Altmann, P. Frisch, S. Inoue, *J. Am. Chem. Soc.* **2019**, *141*, 13536–13546.

[14] J. Keuter, K. Schwedtmann, A. Hepp, K. Bergander, O. Janka, C. Doerenkamp, H. Eckert, C. Mück-Lichtenfeld, F. Lips, *Angew. Chem. Int. Ed.* **2017**, *56*, 13866–13871; *Angew. Chem.* **2017**, *129*, 14054–14059.

[15] Deposition Numbers 1952331 (for **1**), 1952332 (for **2**), 1996479 (for **3**), 1996475 (for **4**), 1996476 (for **5**), 1996477 (for **6**), and 1996478 (for **7**) contain the supplementary crystallographic data for this paper. These data are provided free of charge by the joint Cambridge Crystallographic Data Centre and Fachinformationszentrum Karlsruhe Access Structures service www.ccdc.cam.ac.uk/structures.

[16] a) J. Tao, J. P. Perdew, V. N. Staroverov, G. E. Scuseria, *Phys. Rev. Lett.* **2003**, *91*, 146401; b) S. Grimme, J. Antony, S. Ehrlich, H. Krieg, *J. Chem. Phys.* **2010**, *132*, 154104; c) S. Grimme, S. Ehrlich, L. Goerigk, *J. Comput. Chem.* **2011**, *32*, 1456–1465; d) F. Weigend, R. Ahlrichs, *Phys. Chem. Chem. Phys.* **2005**, *7*, 3297–3305.

[17] a) L. Noodleman, *J. Chem. Phys.* **1981**, *74*, 5737–5743; b) L. Noodleman, E. R. Davidson, *Chem. Phys.* **1986**, *109*, 131–143.

[18] a) Y. Heider, N. E. Poitiers, P. Willmes, K. I. Leszczyńska, V. Huch, D. Scheschkewitz, *Chem. Sci.* **2019**, *10*, 4523–4530; b) K. Abersfelder, A. J. P. White, R. J. F. Berger, H. S. Rzepa, D. Scheschkewitz, *Angew. Chem. Int. Ed.* **2011**, *50*, 7936–7939; *Angew. Chem.* **2011**, *123*, 8082–8086.

[19] T. Matsuno, M. Ichinohe, A. Sekiguchi, *Angew. Chem. Int. Ed.* **2002**, *41*, 1575–1577; *Angew. Chem.* **2002**, *114*, 1645–1647.

[20] a) J. B. Lambert, S. Zhang, *J. Chem. Soc. Chem. Commun.* **1993**, 383–384; b) J. B. Lambert, S. Zhang, S. M. Ciro, *Organometallics* **1994**, *13*, 2430–2443.

[21] J. B. Lambert, Y. Zhao, *Angew. Chem. Int. Ed. Engl.* **1997**, *36*, 400–401; *Angew. Chem.* **1997**, *109*, 389–391.

[22] R. F. W. Bader, *Atoms in Molecules—A Quantum Theory*, Oxford University Press, Oxford, **1990**.

[23] a) P. V. R. Schleyer, C. Maerker, A. Dransfeld, H. Jiao, N. R. J. van Eikema Hommes, *J. Am. Chem. Soc.* **1996**, *118*, 6317–6318; b) Z. Chen, C. S. Wannere, C. Corminboeuf, R. Puchta, P. V. R. Schleyer, *Chem. Rev.* **2005**, *105*, 3842–3888.

[24] E. D. Glendening, A. E. Reed, J. E. Carpenter, F. Weinhold, A. E. Reed, R. B. Weinstock, F. Weinhold, *J. Chem. Phys.* **1985**, *83*, 735–746.

[25] a) P. P. Power, *Chem. Rev.* **1999**, *99*, 3463–3504; b) A. Sekiguchi, V. Y. Lee, *Chem. Rev.* **2003**, *103*, 1429–1448.

[26] a) A. Sekiguchi, T. Matsuno, M. Ichinohe, *J. Am. Chem. Soc.* **2000**, *122*, 11250–11251.

[27] K. Takanashi, V. Y. Lee, T. Yokoyama, A. Sekiguchi, *J. Am. Chem. Soc.* **2009**, *131*, 916–917.

[28] D. Scheschkewitz, *Angew. Chem. Int. Ed.* **2005**, *44*, 2954–2956; *Angew. Chem.* **2005**, *117*, 3014–3016.

[29] M. Kaftory, M. Kapon, M. Botoshansky, *The Chemistry of Organic Silicon Compounds, Vol. 2* (Eds.: Z. Rappoport, Y. Apeloig), Wiley, Chichester, **1998**.

[30] G. Lee, R. West, T. Müller, *J. Am. Chem. Soc.* **2003**, *125*, 8114–8115.

[31] A. E. Reed, R. B. Weinstock, F. Weinhold, *J. Chem. Phys.* **1985**, *83*, 735–746.

[32] S. Inoue, M. Ichinohe, T. Yamaguchi, A. Sekiguchi, *Organometallics* **2008**, *27*, 6056–6058.

[33] K. Wiberg, *Tetrahedron* **1968**, *24*, 1083–1096.

[34] C. Boehme, G. Frenking, *J. Am. Chem. Soc.* **1996**, *118*, 2039–2046.

[35] a) X.-Q. Xiao, H. Zhao, Z. Xu, G. Lai, X.-L. He, Z. Li, *Chem. Commun.* **2013**, *49*, 2706–2708; b) M. Haas, A. Knoechl, T. Wiesner, A. Torvisco, R. Fischer, C. Jones, *Organometallics* **2019**, *38*, 4158–4170.

[36] S. Inoue, J. D. Epping, E. Irran, M. Driess, *J. Am. Chem. Soc.* **2011**, *133*, 8514–8517.

[37] a) T. Nukazawa, T. Kosai, S. Honda, S. Ishida, T. Iwamoto, *Dalton Trans.* **2019**, *48*, 10874–10880; b) M. Ichinohe, Y. Arai, A. Sekiguchi, N. Takagi, S. Nagase, *Organometallics* **2001**, *20*, 4141–4143; c) A. Sekiguchi, M. Ichinohe, R. Kinjo, *Bull. Chem. Soc. Jpn.* **2006**, *79*, 825–832; d) T. Iwamoto, T. Abe, S. Ishida, C. Kabuto, M. Kira, *J. Organomet. Chem.* **2007**, *692*, 263–270.

[38] a) A. Sekiguchi, T. Tanaka, M. Ichinohe, K. Akiyama, S. Tero-Kubota, *J. Am. Chem. Soc.* **2003**, *125*, 4962–4963; b) J. Ohshita, N. Honda, K. Nada, T. Iida, T. Mihara, Y. Matsuo, A. Kunai, A. Naka, M. Ishikawa, *Organometallics* **2003**, *22*, 2436–2441; c) K. Hirotsu, T. Higuchi, M. Ishikawa, H. Sugisawa, M. Kumada, *Chem. Commun.* **1982**, 726–727; d) S. Yao, Y. Xiong, C. van Wullen, M. Driess, *Organometallics* **2009**, *28*, 1610–1612; e) S. Yao, C. van Wuellen, X.-Y. Sun, M. Driess, *Angew. Chem. Int. Ed.* **2008**, *47*, 3250–3253; *Angew. Chem.* **2008**, *120*, 3294–3297; f) D. Gau, R. Rodriguez, T. Kato, N. Saffon-Merceron, A. Baceiredo, *J. Am. Chem. Soc.* **2010**, *132*, 12841–12843; g) F. Lips, A. Mansikkamäki, J. C. Fettinger, H. M. Tuononen, P. P. Power, *Organometallics* **2014**, *33*, 6253–6258; h) A. V. Protchenko, M. P. Blake, A. D. Schwarz, C. Jones, P. Mountford, S. Aldridge, *Organometallics* **2015**, *34*, 2126–2129.

[39] a) S. Ishida, T. Iwamoto, M. Kira, *Heteroat. Chem.* **2011**, *22*, 432–437; b) R. Rodriguez, D. Gau, T. Kato, N. Saffon-Merceron, A. De Cozar, F. P. Cossio, A. Baceiredo, *Angew. Chem. Int. Ed.* **2011**, *50*, 10414–10416; *Angew. Chem.* **2011**, *123*, 10598–10600; c) D. Wendel, W. Eisenreich, C. Jandl, A. Pothig, B. Rieger, *Organometallics* **2016**, *35*, 1–4.

[40] a) Y. Zhao, D. G. Truhlar, *J. Phys. Chem. A* **2005**, *109*, 5656–5667; b) S. Grimme, J. G. Brandenburg, C. Bannwarth, A. Hansen, *J. Chem. Phys.* **2015**, *143*, 054107; c) A. Klamt, *J. Phys. Chem.* **1995**, *99*, 2224–2235.

[41] T. Nukazawa, T. Iwamoto, *Dalton Trans.* **2020**, *49*, 16728–16735.

[42] a) M. Kira, T. Iwamoto, C. Kabuto, *J. Am. Chem. Soc.* **1996**, *118*, 10303–10304; b) N. Wiberg, H. Auer, H. Nöth, J. Knizek, K. Polborn, *Angew. Chem. Int. Ed.* **1998**, *37*, 2869–2872; *Angew. Chem.* **1998**, *110*, 3030–3033; c) N. Wiberg, W. Niedermayer, H. Nöth, M. Warchhold, *Z. Anorg. Allg. Chem.* **2001**, *627*, 1717–1722; d) A. Sekiguchi, T. Matsuno, M. Ichinohe, *J. Am. Chem. Soc.* **2001**, *123*, 12436–12437; e) C. B. Yildiz, K. I. Leszczyńska, S. González-Gallardo, M. Zimmer, A. Azizoglu, T. Biskup, C. W. M. Kay, V. Huch, H. S. Rzepa, D. Scheschkewitz, *Angew. Chem. Int. Ed.* **2020**, *59*, 15087–15092.

[43] a) Y. Naruse, J. Ma, K. Takeuchi, T. Noharaa, S. Inagaki, *Tetrahedron* **2006**, *62*, 4491–4497; b) Y. Naruse, J. Mab, S. Inagakia, *Tetrahedron Lett.* **2001**, *42*, 6553–6556.

[44] T. Iwamoto, M. Tamura, C. Kabuto, M. Kira, *Science* **2000**, *290*, 504–506.